

# Quarterly Technical Report

## Selected Energy Epitaxial Deposition and Low Energy Electron Microscopy of AlN, GaN and SiC Thin Films

Supported under Grant #N00014-95-1-0122  
Office of the Chief of Naval Research  
Report for the period 7/1/95-9/30/95



R. F. Davis, H. H. Lamb and I. S. T. Tsong\*,  
E. Bauer\*, R. B. Doak\*, J. L. Edwards\*, N. Freed\*, S. Horch\*,  
C. Linsmeier\*, M. Meloni\*, K. E. Schmidt\*, J. Sumakeris and V. Torres\*  
Materials Science and Engineering Department  
North Carolina State University  
Campus Box 7907  
Raleigh, NC 27695-7907

and  
\*Department of Physics and Astronomy  
Arizona State University  
Tempe, AZ 85287-1504

September, 1995

DISTRIBUTION STATEMENT A

Approved for public release;  
Distribution Unlimited

19951019 000

DTIC QUALITY INSPECTED 5

## REPORT DOCUMENTATION PAGE

Form Approved  
OMB No. 0704-0188

Public reporting burden for this collection of information is estimated to average 1 hour per response, including the time for reviewing instructions, searching existing data sources, gathering and maintaining the data needed, and completing and reviewing the collection of information. Send comments regarding this burden estimate or any other aspect of this collection of information, including suggestions for reducing this burden to Washington Headquarters Services, Directorate for Information Operations and Reports, 1215 Jefferson Davis Highway, Suite 1204, Arlington, VA 22202-4302, and to the Office of Management and Budget Paperwork Reduction Project (0704-0188), Washington, DC 20503.

1. AGENCY USE ONLY (Leave blank)		2. REPORT DATE September, 1995	3. REPORT TYPE AND DATES COVERED Quarterly Technical 7/1/95-9/30/95
4. TITLE AND SUBTITLE Selected Energy Epitaxial Deposition and Low Energy Electron Microscopy of AlN, GaN, and SiC Thin Films			5. FUNDING NUMBERS 1213801---01 312 N00179 N66020 4B855
6. AUTHOR(S) R. F. Davis, H. H. Lamb and I. S. T. Tsong			
7. PERFORMING ORGANIZATION NAME(S) AND ADDRESS(ES) North Carolina State University Hillsborough Street Raleigh, NC 27695			8. PERFORMING ORGANIZATION REPORT NUMBER  N00014-95-1-0122
9. SPONSORING/MONITORING AGENCY NAME(S) AND ADDRESS(ES) Sponsoring: ONR, Code 312, 800 N. Quincy, Arlington, VA 22217-5660 Monitoring: Administrative Contracting Officer, Regional Office Atlanta Regional Office Atlanta, 101 Marietta Tower, Suite 2805 101 Marietta Street Atlanta, GA 30323-0008			10. SPONSORING/MONITORING AGENCY REPORT NUMBER
11. SUPPLEMENTARY NOTES			
12a. DISTRIBUTION/AVAILABILITY STATEMENT  Approved for Public Release; Distribution Unlimited			12b. DISTRIBUTION CODE
13. ABSTRACT (Maximum 200 words)  At North Carolina State University, GaN films have been deposited on Al <sub>2</sub> O <sub>3</sub> (0001) substrates at 550°C using triethylgallium and NH <sub>3</sub> seeded free jets. An NH <sub>3</sub> to triethylgallium ratio of 151 yielded the best GaN films in this configuration. Experiments to determine the optimal skimmer locations have been performed in anticipation of the future employment of skimmed, differentially pumped beams. The assembly of a new deposition system supporting two skimmed and differentially pumped supersonic beams and associated <i>in-situ</i> characterization using reflection high energy electron diffraction and on-line x-ray photoelectron spectroscopy has made excellent progress. At Arizona State University, construction of a selected energy epitaxial deposition (SEED) apparatus is still in progress. The supersonic molecular beam source is under construction and the associated gas manifold has been completed. The UHV chambers for the dual Colutron ion-beam system have been completed and are being assembled. Deposition of AlN and GaN films using an effusive source and activated nitrogen species via microwave discharge has been conducted in a test chamber for the purpose of interfacing to the LEEM for <i>in situ</i> real-time observation of film growth. Various schemes of preparing the 6H-SiC(0001) substrates were explored and the resulting surfaces were studied by LEED/LEEM. Removal of the scratches on the SiC substrate surfaces remains a challenging problem.			
14. SUBJECT TERMS gallium nitride, GaN, aluminum nitride, AlN, seeded free jets, selected energy epitaxial deposition, supersonic molecular beams, Colutron, microwave discharge, silicon carbide, SiC, cleaning, surfaces			15. NUMBER OF PAGES 32
			16. PRICE CODE
17. SECURITY CLASSIFICATION OF REPORT UNCLAS	18. SECURITY CLASSIFICATION OF THIS PAGE UNCLAS	19. SECURITY CLASSIFICATION OF ABSTRACT UNCLAS	20. LIMITATION OF ABSTRACT SAR

## Table of Contents

I.	Introduction	1
II.	Deposition of GaN Thin Films via Supersonic Jets and Design and Construction of New Deposition System	4
III.	Deposition of GaN Thin Films Using Activated NH <sub>3</sub> from a Microwave Cavity	16
IV.	Design of a Supersonic Molecular Beam Source for <i>in situ</i> Growth of AlN and GaN Layers for Low Energy Electron Microscopy (LEEM)	22
V.	Design of System for Deposition of GaN and SiC Films by Dual Colutron Ion Beams	24
VI.	Surface Microstructure and Crystal Structure of 6H-SiC(0001) Substrates for Nitride Film Growth	27
VII.	Distribution List	32

Accession For		
NTIS	CRA&I	<input checked="" type="checkbox"/>
DTIC	TAB	<input type="checkbox"/>
Unannounced		<input type="checkbox"/>
Justification _____		
By _____		
Distribution /		
Availability Codes		
Dist	Avail and/or Special	
A-1		

## I. Introduction

The realized and potential electronic applications of AlN, GaN and SiC are well known. Moreover, a continuous range of solid solutions and pseudomorphic heterostructures of controlled periodicities and tunable bandgaps from 2.3 eV (3C-SiC) to 6.3 eV (AlN) have been produced at North Carolina State University (NCSU) and elsewhere in the GaN-AlN and AlN-SiC systems. The wide bandgaps of these materials and their strong atomic bonding have allowed the fabrication of high-power, high-frequency and high-temperature devices. However, the high vapor pressures of N and Si in the nitrides and SiC, respectively, force the use of low deposition temperatures with resultant inefficient chemisorption and reduced surface diffusion rates. The use of these low temperatures also increases the probability of the uncontrolled introduction of impurities as well as point, line and planar defects which are likely to be electrically active. An effective method must be found to routinely produce intrinsic epitaxial films of AlN, GaN and SiC having low defect densities.

Recently, Ceyer [1, 2] has demonstrated that the barrier to dissociative chemisorption of a reactant upon collision with a surface can be overcome by the translational energy of the incident molecule. Ceyer's explanation for this process is based upon a potential energy diagram (Fig. 1) similar to that given by classical transition-state theory (or activated-complex theory) in chemical kinetics. The dotted and dashed lines in Fig. 1 show, respectively, the potential wells for molecular physisorption and dissociative chemisorption onto the surface. In general, there will be an energy barrier to overcome for the atoms of the physisorbed molecule to dissociate and chemically bond to the surface. Depending upon the equilibrium positions and well depths of the physisorbed and chemisorbed states, the energy of the transition state  $E^*$  can be less than zero or greater than zero. In the former case, the reaction proceeds spontaneously. In the latter case, the molecule will never proceed from the physisorbed state (the precursor state) to the chemisorbed state unless an additional source of energy can be drawn upon to surmount the barrier. This energy can only come from either (1) the thermal energy of the surface, (2) stored internal energy (rotational and vibrational) of the molecule, or (3) the incident translational kinetic energy of the molecule. Conversion of translational kinetic energy into the required potential energy is the most efficient of these processes. Moreover, by adjusting the kinetic energy,  $E_i$ , of the incoming molecule, it is possible to turn off the reaction ( $E_i < E^*$ ), to tailor the reaction to just proceed ( $E_i = E^*$ ), or to set the amount of excess energy to be released ( $E_i > E^*$ ). The thrust of the present research is to employ these attributes of the beam translational energy to tune the reaction chemistry for wide bandgap semiconductor epitaxial growth.

The transition state,  $E^*$ , is essentially the activation energy for dissociation and chemisorption of the incident molecules. Its exact magnitude is unknown, but is most certainly

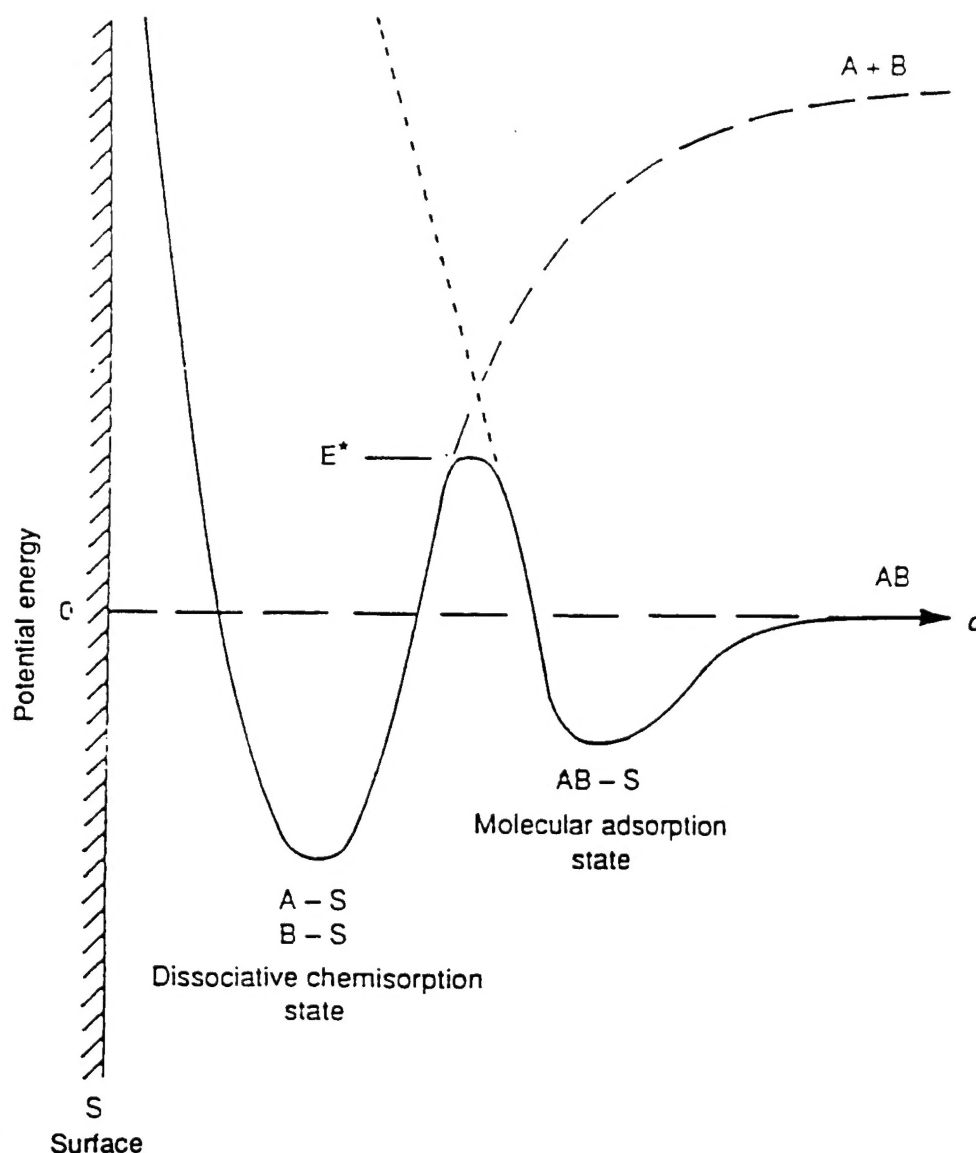


Figure 1. Schematic potential energy diagram of an activated surface reaction involving a molecularly physisorbed precursor state [from Ref. 1].

lower than the dissociation energy of the free molecule. It does not necessarily follow, however, that any kinetic energy above  $E^*$  will promote high-quality epitaxial growth of GaN. One must take into consideration another energy threshold,  $E_d$ , beyond which the kinetic energy of the incident flux will cause damage to the epitaxial film being synthesized. A typical  $E_d$  threshold value is approximately five times the bandgap of the crystal and in the case of GaN,  $E_d \approx 18$  eV.

From the above consideration, it is clear that the key to high quality epitaxial growth is to be able to tune the energy of the incoming flux species over a range of energies defined by the window between  $E^*$  and  $E_d$ . Since the window is quite restrictive, i.e. 1-20 eV, it is essential

that the energy spread of the flux species must be small, i.e. the flux species should ideally be monoenergetic. To this end, we employ Selected Energy Epitaxial Deposition (SEED) systems for the growth of AlN, GaN and SiC wide bandgap semiconductors. The SEED systems are of two types: (1) a seeded-beam supersonic free-jet (SSJ) and (2) a dual ion-beam Colutron. Both these SEED systems have the desirable property of a narrow energy spread of  $\leq 1$  eV.

Epitaxial growth using the seeded-beam SSJ involves a close collaboration between investigators at NCSU and Arizona State University (ASU). At ASU, the SSJ is interfaced directly into a low-energy electron microscope (LEEM) for the conduct of *in situ* studies of the nucleation and growth of epitaxial layers; while at NCSU, the SSJ systems are used to grow device-quality AlN, GaN and SiC for real applications. Exchanges in personnel (students) and information between the two groups ensures the achievement of desired results. The additional thin film growth experiments using dual-beam Colutrons and the theoretical studies referred to in this report are primarily conducted at ASU.

The research conducted in this reporting period and described in the following sections has been concerned with (1) deposition of GaN and AlN films using seeded free jets and effusive sources coupled with activate nitrogen species via microwave discharge, (2) the design of new III-V nitride and SiC deposition systems involving supersonic beams, dual Colutron ion-beams, and microwave discharge processes, and (3) preparation of 6H-SiC substrate surfaces. The following individual sections detail the procedures, results, discussions of these results, conclusions and plans for future research. Each subsection is self-contained with its own figures, tables and references.

1. S. T. Ceyer, Langmuir **6**, 82 (1990).
2. S. T. Ceyer, Science **249**, 133 (1990).

## II. Deposition of GaN Thin Films via Supersonic Jets and Design and Construction of New Deposition System

### A. Introduction

The III-V nitrides of AlN and GaN are presently receiving great attention as researchers and microelectronic device manufacturers attempt to exploit the optoelectronic properties of these materials. Research into SiC film deposition and device fabrication is also progressing rapidly due to several applications of the material. Silicon carbide is used in the fabrication of high-power, -temperature and -frequency devices in addition to blue light emitting diodes [1]. Silicon carbide is also one of the most suitable substrates for the epitaxial deposition of III-V nitride films. Typically, thin films of all three materials may be deposited via chemical vapor deposition at elevated temperatures. It is very desirable to lower deposition temperatures in pursuit of the lower thermal budgets which are necessary to maintain abrupt changes in dopant profiles. Techniques which enable the deposition of thin films of these materials could dramatically advance the availability of several optoelectronic devices.

Selected energy epitaxial deposition (SEED) may serve as a vehicle to reduce the temperatures required to deposit thin films of AlN, GaN and SiC. By seeding a reactant gas molecule in an expanding, high velocity (supersonic) gas stream, a substantial amount of kinetic energy may be "attached" to each reactant molecule. Due to the seeding effect, the heavier reactant molecules achieve hyperthermal velocities with an associated high kinetic energy of up to several eV. When a supersonic molecule impinges on the substrate, the "entrained" energy could serve to drive a film deposition reaction at relatively low temperature. This is particularly interesting in cases where one source molecule reacts fairly readily while another is more stable. This is the case for the deposition of GaN from triethylgallium (TEGa) and  $\text{NH}_3$ . Although TEGa will react at low temperatures,  $\text{NH}_3$  is fairly stable and a significant deposition rate requires higher deposition temperatures. An  $\text{NH}_3$  seeded beam could serve as an activated N source to permit the deposition of GaN films at lower temperatures.

This report documents progress and results in the application of seeded supersonic jets to the deposition of GaN films. During this reporting period, GaN films were deposited using TEGa and  $\text{NH}_3$  in a free standing supersonic beam deposition chamber. A more capable deposition system, with an *in-situ* analysis capability is currently under construction and progress toward the commissioning of the new system is summarized.

### B. Experimental

*Deposition System.* A schematic representation of the reactor is presented in Fig. 1. The system setup was altered from the previous report as an unheated free jet TEGa source was installed for film deposition. Samples were installed into the reactor via a simple load lock. Substrates were then heated by a quartz-halogen bulb to a maximum temperature of 650°C and



the nozzle heater could attain 600°C. The pumping system on the source (right) side of the reactor achieved  $\approx 1900$  liters/sec. while the deposition (left) side pumping system operated at  $\approx 950$  liters/sec. When operated in the free jet configuration, without a skimmer installed, a total gas flow of 300 sccm resulted in a chamber pressure of  $\approx 1$ mtorr.

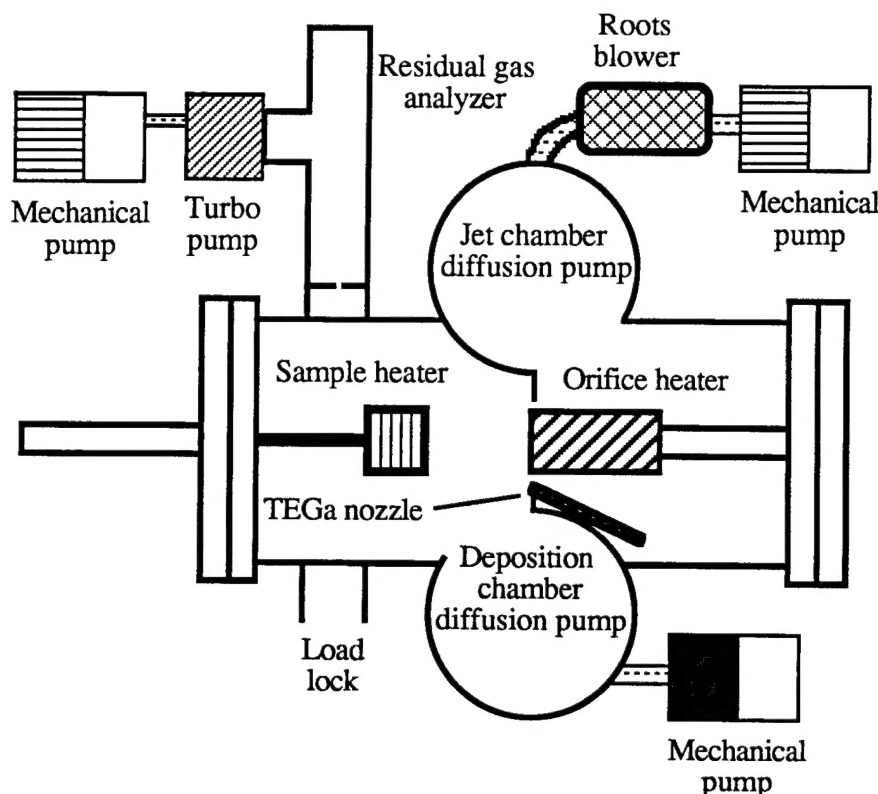


Figure 1. Currently active supersonic jet deposition system configured for deposition.

A short experimental series was performed to examine the effect of skimmer position on reactive beam intensity. For this study, the system was configured as shown in Fig. 2. In this case, an electroformed skimmer was installed and the RGA was positioned to be directly in the skimmed beam path. With the beam flag retracted, the RGA could measure the "beam pressure." When the beam flag was inserted, it blocked the beam and the RGA could measure the background pressure in the chamber. The ratio of the two pressures was examined at several jet-skimmer spacings.

*Substrate Preparation.*  $\text{Al}_2\text{O}_3(0001)$  substrates were cleaned via a multiple step process. Firstly, the samples were successively ultrasonically cleaned in trichloroethylene, acetone and methanol. After water rinsing, the samples were immersed in a 70°C, 50:50 mixture of  $\text{H}_3\text{PO}_4$  and  $\text{H}_2\text{SO}_4$  for 5 minutes. After water rinsing, the substrates were finally immersed in a 10% HF solution immediately prior to installation in the reactor.



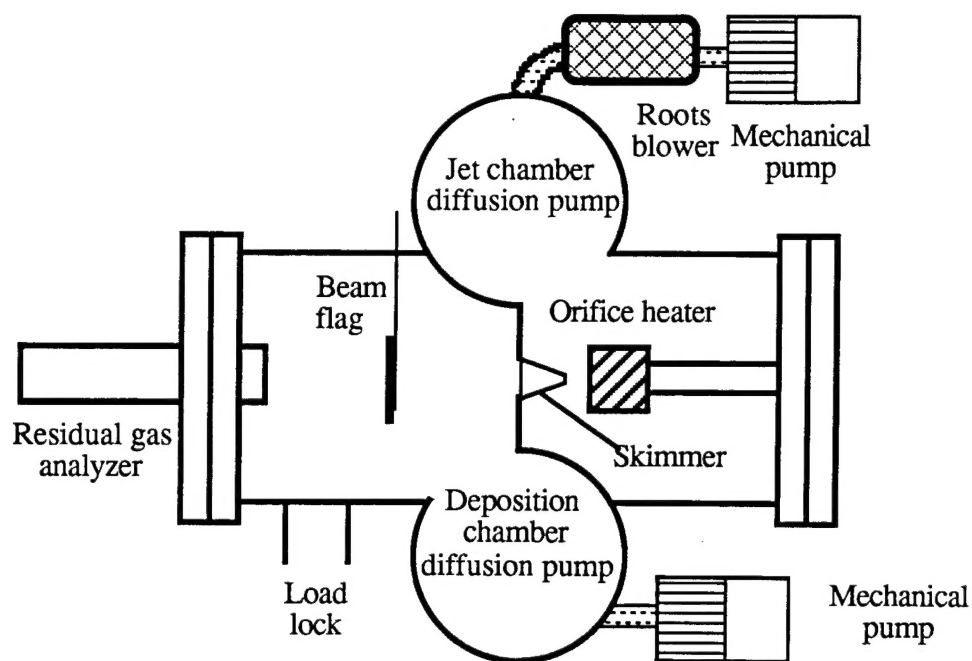


Figure 2. Currently active supersonic jet deposition system configured for beam intensity measurements.

*Film Deposition.* After installation in the reactor, the samples were heated to the deposition temperature under a 5%  $\text{NH}_3$  in He gas flow. After reaching the specified deposition temperature, the TEGa flow was initiated and maintained for the duration of the deposition run. Upon completion, the TEGa flow was stopped and the sample cooled to  $<200^\circ\text{C}$  under the  $\text{NH}_3/\text{He}$  gas flux. The ranges of significant GaN deposition conditions explored in this research are listed in Table I.

Table I. Ranges of GaN Deposition Conditions.

Parameter	Value
Substrate temperature	$540^\circ$ to $580^\circ\text{C}$
Orifice diameter	100 to 200 $\mu\text{m}$
Orifice pressure	400 to 1000 Torr
Orifice temperature	$510^\circ\text{C}$
Orifice gas	5% $\text{NH}_3$ in He
TEGa bubbler temperature	$-5$ to $10^\circ\text{C}$
TEGa bubbler pressure	300 to 800 Torr
TEGa carrier	20 to 40 sccm He
$\text{NH}_3/\text{TEGa}$ ratio	$\approx 75$ to $\approx 300$

### C. Results and Discussion

*Skimmed Beam Intensity Measurements.* During beam intensity measurements, the mass spectrometer, skimmer and beam flag were arranged as detailed in Fig. 3. With this arrangement, the mass spectrometer could either directly sample the beam intensity with the flag retracted, or the background pressure could be measured with the flag inserted. The ratio of the two pressures was determined at  $X_s$  values of 5, 10, 20 and 40 mm and the resultant calculations are presented in Table II. In this series, He was expanded from a 1000 Torr stagnation pressure into a  $2 \times 10^{-3}$  Torr vacuum through a  $100 \mu\text{m}$  diameter orifice. Equation 1 [2] gives a mach disc distance  $X_M$  of 47 mm. Therefore, all of the skimmer positions studied in this series should be within the mach disc.

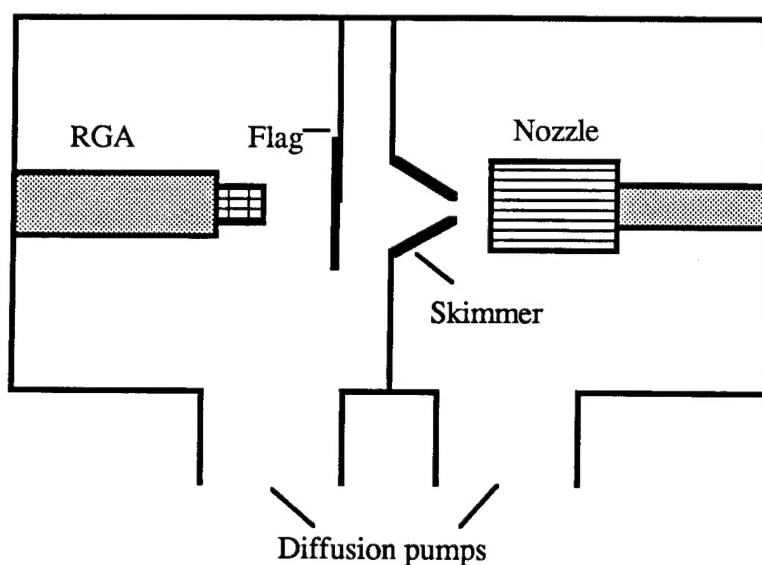


Figure 3. Experimental configuration for beam intensity measurements

Table II. Beam Intensity Ratio Measurements.

$X_s$	Beam Pressure	Background Pressure	Intensity Ratio
5 mm	$2.8 \times 10^{-5}$ Torr	$2.1 \times 10^{-5}$ Torr	1.33
10 mm	$1.6 \times 10^{-5}$ Torr	$9.2 \times 10^{-6}$ Torr	1.74
20 mm	$9.4 \times 10^{-6}$ Torr	$4.5 \times 10^{-6}$ Torr	2.1
40 mm	$4.8 \times 10^{-6}$ Torr	$2.3 \times 10^{-6}$ Torr	2.1

$$X_M = 0.67 D \sqrt{\frac{P_0}{P_I}} \quad (1)$$

Equation 2 [2] can be used to determine the optimal skimmer location dependent upon the pressure drop and orifice size. For these conditions, equation yields  $X_S = 21 \text{ mm}$  ( $\lambda_0 = 1 \text{ }\mu\text{m}$ ). This is in fairly good agreement with the observed behavior, although the absolute beam intensity is very low at this distance. For this system, an  $X_S$  value of  $\approx 10 \text{ mm}$  seem to give a better balance between the absolute beam intensity and the beam intensity ratio.

$$X_S = 0.125 \left[ \left( \frac{d}{\lambda_0} \right) \left( \frac{P_0}{P_I} \right) \right]^{\frac{1}{3}} \quad (2)$$

*Deposition Attempts using a Skimmed  $\text{NH}_3$  Beam and a TEGa Seeded Free Jet.* Attempts to deposit GaN films using a skimmed  $\text{NH}_3$  seeded beam and a TEGa seeded free jet were unsuccessful. Due to system pumping limitations, it was impossible to attain an  $\text{NH}_3$ :TEGa ratio above  $\approx 20$  while maintaining reasonable TEGa flow rates. As a consequence, all of these deposition attempts either resulted in no or very little deposition, or Ga films were deposited. Due to these factors, the deposition of GaN films using independent free jets seeded with either  $\text{NH}_3$  and TEGa was examined.

*Deposition Attempts using  $\text{NH}_3$  and TEGa Seeded Free Jets.* The deposition of GaN films using  $\text{NH}_3$  and TEGa seeded free jets was found to be very sensitive to deposition conditions, most importantly sample position and the  $\text{NH}_3$ :TEGa ratio. As depicted in Fig. 4, there is only a relatively small region in the system within which both reactant fluxes are reasonably uniform. Locating this region was an iterative process that required several deposition runs.

Once the proper deposition position was identified, a series of deposition experiments was conducted to assess the role of the  $\text{NH}_3$ :TEGa ratio on the composition and morphology of any resulting film. The deposition conditions examined are detailed in Table III. The  $\text{NH}_3$  was diluted to 5% in He and all deposition runs lasted approximately 2 hours.

Figures 5-8 are scanning electron micrographs of the films deposited in Run #1-Run #4, respectively. The film depicted in Fig. 5 has the lowest  $\text{NH}_3$ :TEGa ratio (88) in this series and excess Ga is visible as droplets on the film surface. The film in Fig. 6 is relatively uniform while the film in Fig. 7 exhibits larger grains of GaN. Such a development is encouraging as deposition conditions are refined for epitaxial deposition. The last film deposited in this series, pictured in Figure 8 is discontinuous, probably because of the very low TEGa flux to the substrate. An interesting artifact observed on the film deposited in Run #3 is imaged in Figure 9. Several features similar to the one imaged were observed on this film. These tall helical whiskers exhibit clearly visible ledges that are hypothesized to be growth ledges. These

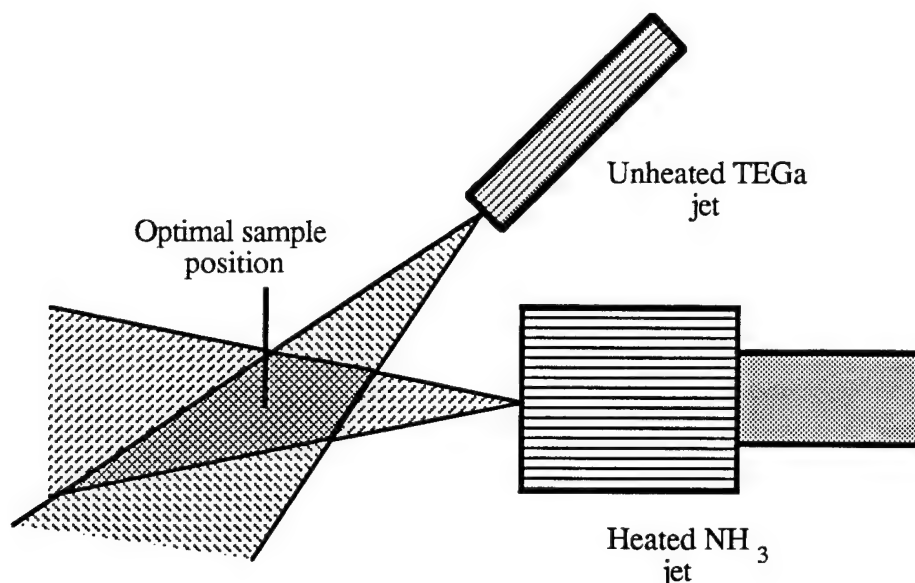


Figure 4. Region of uniform deposition in dual free jet configuration.

Table III. Deposition conditions employed to examine the role of the  $\text{NH}_3$ :TEGa ratio of film characteristics.

Parameter	Run #1	Run #2	Run #3	Run #4
Substrate T	590°C	590°C	590°C	590°C
$\text{NH}_3$ nozzle T	570°C	570°C	570°C	570°C
$\text{NH}_3$ nozzle P	500 Torr	500 Torr	450 Torr	450 Torr
$\text{NH}_3$ flow rate	14 sccm	14 sccm	12.6	12.6
TEGa T	10°C	5°C	0°C	-5°C
TEGa P	700 Torr	700 Torr	700 Torr	700 Torr
TEGa carrier	40 sccm	40 sccm	40 sccm	40 sccm
TEGa flow rate	0.159 sccm	0.116 sccm	0.083 sccm	0.059 sccm
$\text{NH}_3$ :TEGa ratio	88	121	151	213

features are reminiscent of the columnar structure detailed in the previous report and appear to be a consequence of an anisotropic deposition rate resulting from free jet deposition. An Auger electron spectrum taken from the film deposited in Run #3 is presented in Fig. 10. In this spectrum, the major film contaminants are O and C. From this series, an  $\text{NH}_3$ :TEGa ratio of  $\approx 151$  was accepted as an optimal value for the initial refinement of the deposition conditions.

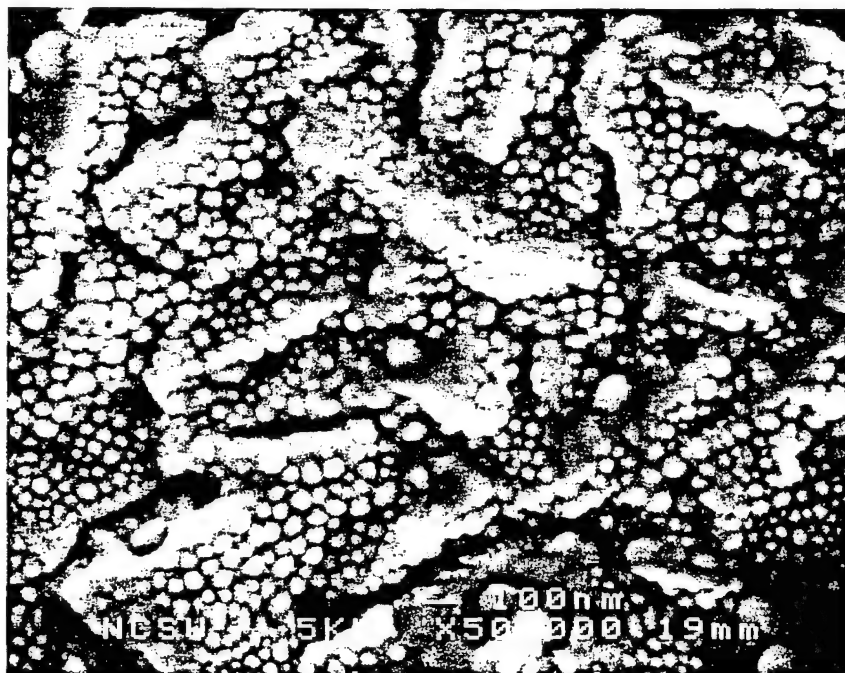


Figure 5. GaN film deposited with an  $\text{NH}_3$ :TEGa ratio of 88.

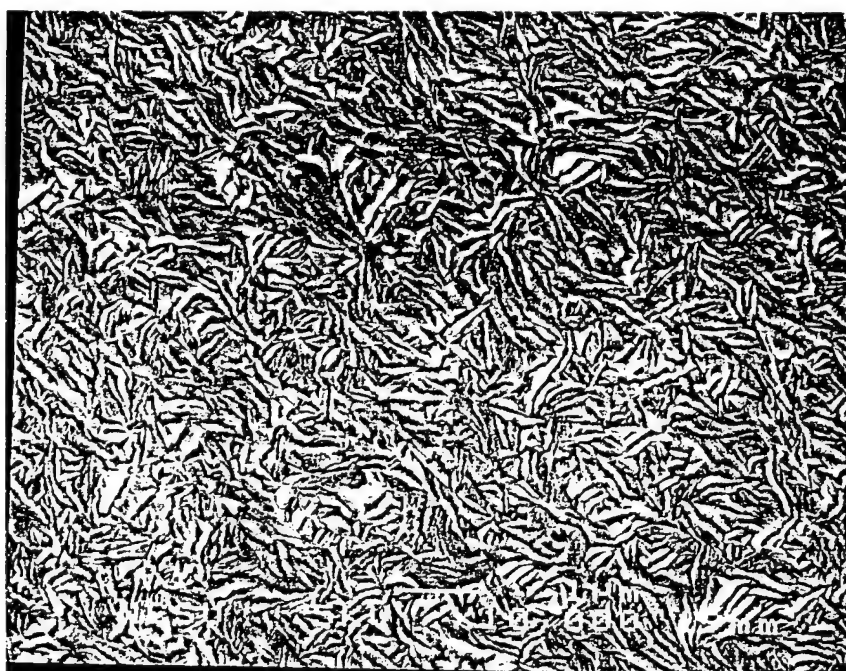


Figure 6. GaN film deposited with an  $\text{NH}_3$ :TEGa ratio of 121.



Figure 7. GaN film deposited with an  $\text{NH}_3$ :TEGa ratio of 151.

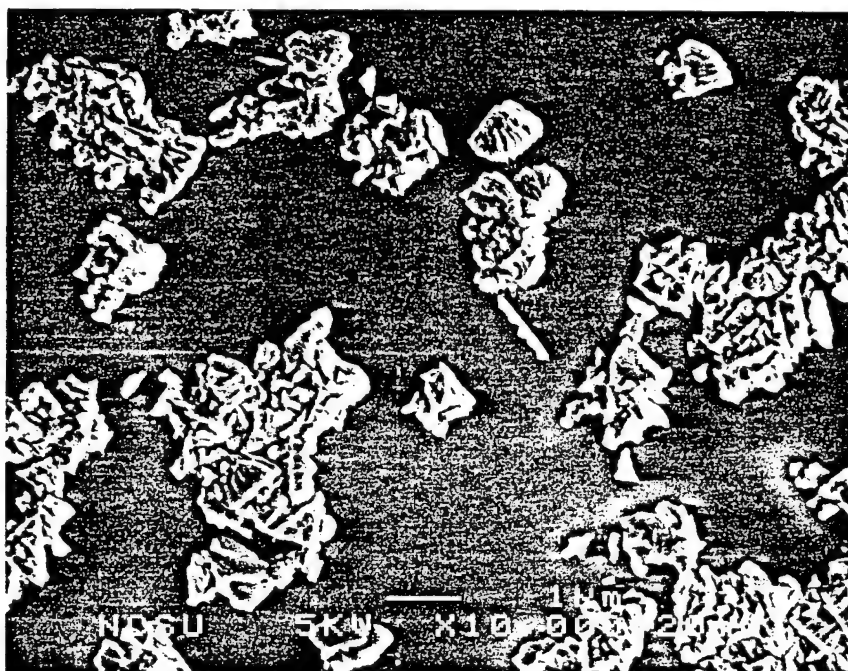


Figure 8. GaN film deposited with an  $\text{NH}_3$ :TEGa ratio of 213.



Figure 9. Helical whisker of GaN film deposited with an  $\text{NH}_3$ :TEGa ratio of 151.

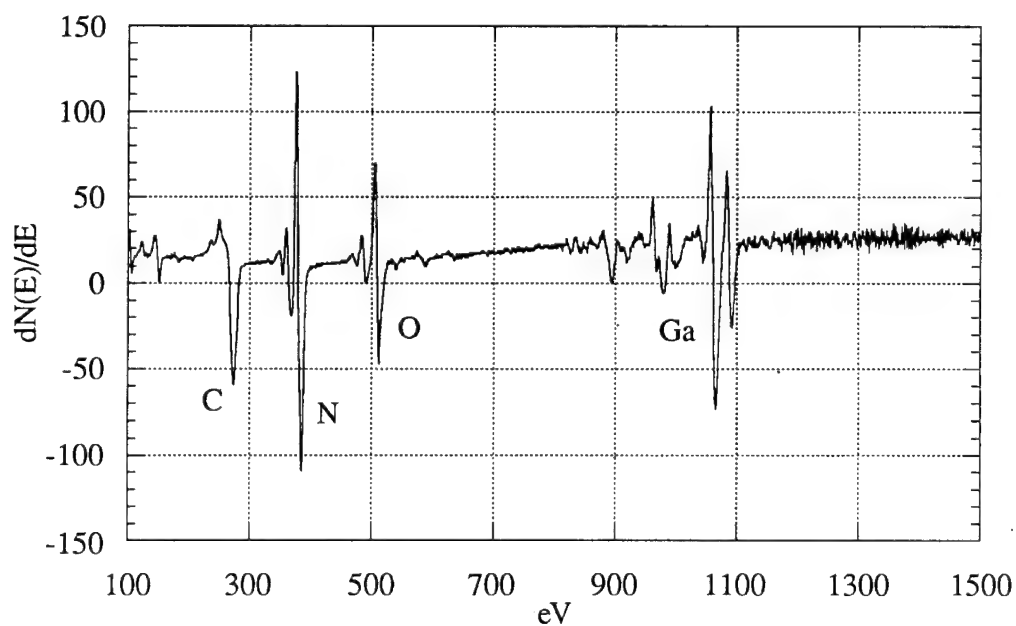


Figure 10. Auger spectrum taken from a GaN film deposited at an  $\text{NH}_3$ :TEGa ratio of 155.



*Progress in Completion of New SEED Facility.* Several major steps in the completion of the new SEED facility have been accomplished in this period. The new system will consist of three chambers, a transfer line and a load lock configure as indicated in Fig. 11. Dual independent seeded free jets will be generated in the source chamber where skimmers will be employed in addition to slits to collimate and differentially pump the beams. The source chamber will also provide mechanisms for chopping the beams for time of flight characterization and for selectively blocking one beam or the other for layer-by-layer deposition.

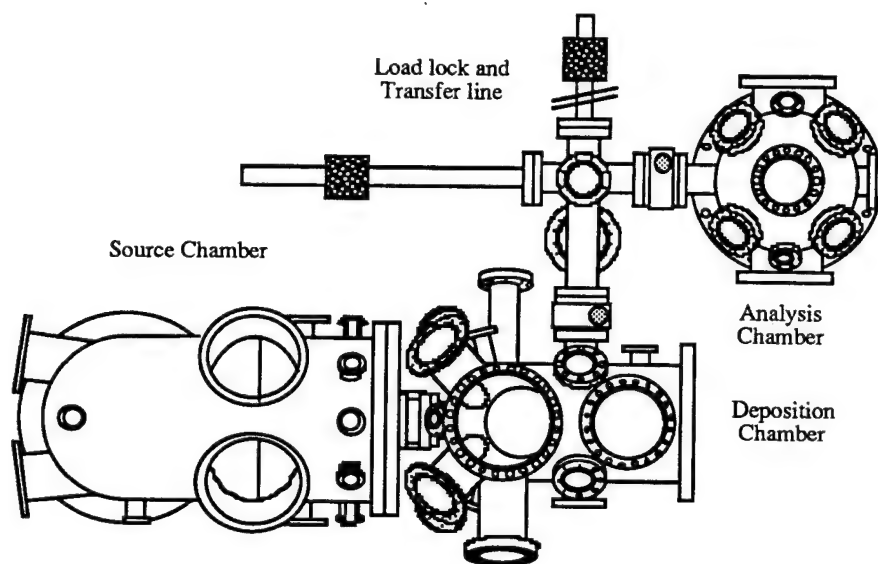


Figure 11. Overhead view of SEED facility currently under construction at NCSU.

The deposition chamber will house the substrate heater and support samples at the coincident spot of the two beams previously mentioned. In addition to the seeded beams, deposition of films may also be accomplished employing evaporation cells or a radio frequency plasma sources that may to be fitted to the deposition chamber. The deposition chamber will be support several analytical capacities, including reflection high energy electron diffraction (RHEED), time of flight and adsorption/desorption studies employing a high sensitivity mass spectrometer, and p-polarized laser reflectance interferometry. Samples may also be analyzed on-line via an *in-vacuo* transfer to an analysis chamber supporting angle dependent x-ray photoelectron spectroscopy (ADXPS).

Several major components of the new facility have arrived and have been verified. The specific materials are assigned to the appropriate chamber:

#### Source Chamber:

- Chamber completed and leak checked.
- Jet manipulators completed and functional.
- All of the pumping system has arrived: Varian VHS-400 and VHS-6 diffusion pumps, Leybold D-30 mechanical pump, Roots blower and backing pump. Only the VHS-400 has yet to be operated.
- Pressure gauges have arrived and have been verified.

#### Deposition Chamber:

- Magnetic bearing-molecular drag combination turbo pump and Fomblinized backing pump have arrived and are operating.
- Pulsed ion counting mass spectrometer has arrived and is operational.
- Pentium 90 computer for TOF measurements is being used to operate the mass spectrometer.
- Titanium sublimation pump system has arrived, but has not been tested.

#### Analysis Chamber:

- Analysis chamber has arrived, but has not been tested.
- XPS system has arrived, but has not been tested.
- Ion pump has arrived and has been tested.
- Air suspension table for analysis chamber has been tested.
- 486-DX2 computer for ADXPS has arrived and is operational.

#### Transfer line and load lock

- Drytel vacuum pump has arrived and is operational.

The following items have been ordered and shipping dates are indicated where available:

- Deposition chamber, Oct. 6.
- Rotatable table for mass spectrometer, Sept. 21.
- Cryopump and evacuated body gate valve for transfer line.
- RHEED system, requisition placed.

#### D. Future Plans

##### Film Deposition in the Existing System.

1. Attempt to improve film morphology by varying  $\text{NH}_3$ :TEGa ration during deposition to use a low ratio to nucleate the films and a high ration for the majority of the deposition.

2. Explore the seeding effects on  $\text{NH}_3$  and TEGa (% dilution, Ar carrier).

Construction of New SEED Facility.

1. Test analysis chamber and XPS system, currently underway.
2. Design high temperature nozzle for source chamber.
3. Design manipulator for analysis chamber.

E. References

1. R. F. Davis, J. Cryst. Growth **137**, 191 (1994).
2. R. Campargue, J. Phys. Chem **88**, 4466 (1984).

### III. Deposition of GaN Thin Films Using Activated $\text{NH}_3$ from a Microwave Cavity

#### A. Introduction

The epitaxial growth of AlN or GaN films at low temperature requires a reactive nitrogen species. In the supersonic nozzle approach this will be obtained by using molecules with a high translational energy. A more conventional approach is to activate the nitrogen prior to adsorption, for example by means of a microwave discharge [1-3]. A microwave cavity and power supply were obtained from NCSU. As we are waiting for the supersonic nozzle to come on line at ASU, we plan to use the LEEM to study nitride growth by the microwave cavity method. Accordingly, we set up a small test chamber to see if we are able to pinpoint the growth parameters necessary for LEEM studies.

#### B. Experimental Procedure

A small vacuum chamber was built containing an effusive Ga (or Al) source (a) and microwave source (b) used to activate a  $\text{NH}_3/\text{Ar}$  mixture as shown in Fig. 1. The gas mixture with a ratio of about 1:1 was introduced to the chamber through a Pyrex glass tube. The gas flow was controlled by a leak valve in the gas line.

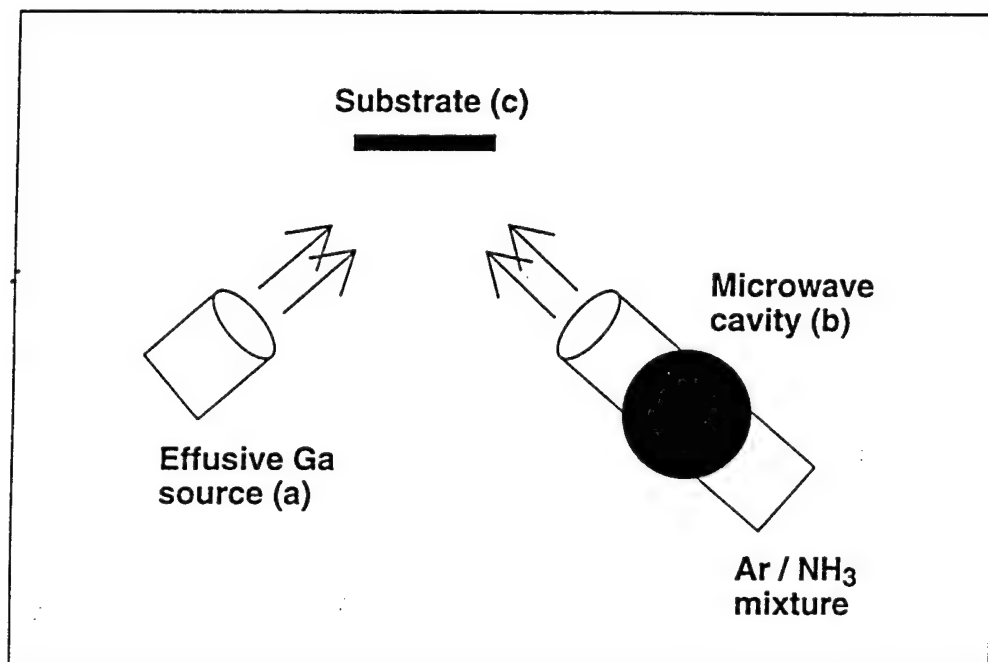


Figure 1. Schematic drawing of the test chamber: (a) Effusive Ga source, (b) microwave cavity sitting on the Pyrex tube, (c) sample. The angle between the Ga source and the microwave is  $72^\circ$ . The three other ports of the deposition chamber are used for two vacuum gauges and a window for the pyrometer reading of the sample temperature.

In order to operate the reaction chamber at pressures  $\leq 10^{-5}$  mbar (the highest operating pressure for the LEEM), a 0.1 mm diameter aperture was inserted into the 12 mm diameter Pyrex tube which formed part of the gas line. The microwave cavity was placed on the outside of the tube such that the discharge took place in the high pressure region of the tube, i.e. between the leak valve and the aperture. The cavity was positioned as close to the aperture as possible. Activated species resulting from the cracking of the ammonia exited from the discharge region (i.e., the high-pressure region) through the aperture into the lower-pressure region of the chamber containing the substrate. The distance from the aperture to the substrate was about 20 cm which was short enough to keep the recombination rate of the activated species low. At  $10^{-4}$  mbar, the mean free path of Ar is about 50 cm. As the objective of the experiment is to test whether Ga will react with N to form a film for the purpose of LEEM studies, the nature of the substrate is unimportant and we chose Si(100) wafers.

The base pressure in the chamber was typically  $\leq 10^{-8}$  mbar which was achieved without baking the system. The films grown in the chamber were removed and transferred to a tandem accelerator where they were analyzed by Rutherford backscattering spectrometry (RBS).

The carrier gas used in our microwave was Ar which gave a very stable discharge. As nitrogen source gas we tried  $N_2$  [1,3] and  $NH_3$  [2]. We decided to use  $NH_3$  because it appeared to be more reactive [4]. Moreover, at lower pressures the microwave discharge could be maintained more easily with a  $NH_3$ /Ar mixture. A residual gas analyzer was mounted in the chamber to analyze the gas composition and content.

### C. Results

The most important parameters in the growth of GaN films were: (a) substrate temperature, (b) total pressure in the reaction chamber, (c)  $NH_3$ /Ga ratio (i.e., N/Ga ratio), and (d) microwave power. The composition of the films was measured using RBS.

We first grew films at room temperature. Figure 2 shows the RBS spectrum of an AlN film grown on Si(100). Due to the similar masses of Al and Si, their surface peaks can overlap in the RBS spectrum. Light elements have a smaller scattering cross-section. Therefore N gives only a small backscattering signal on a large Si background. In order to enhance the N signal, this and the following spectra have been obtained under nuclear resonance conditions, which for the  $He^{2+}$  ions used in the RBS measurements occur at an ion energy of around 3.7 MeV. Under these conditions, the N peak can clearly be seen on the top of the Si signal. The O peak is caused by the oxidation of Al during the sample transfer in air.

Further experiments were carried out at higher substrate temperatures. Under these conditions, however, the growth rate decreases drastically. One way to overcome this problem is to work at high N overpressure [3]. In order to be compatible with the LEEM, however, we have to keep the total pressure in the reaction chamber well below  $10^{-4}$  mbar. We found that the

final Ga/N ratio depended critically on the substrate temperature which greatly influences the sticking probability of Ga as the Si Substrate.

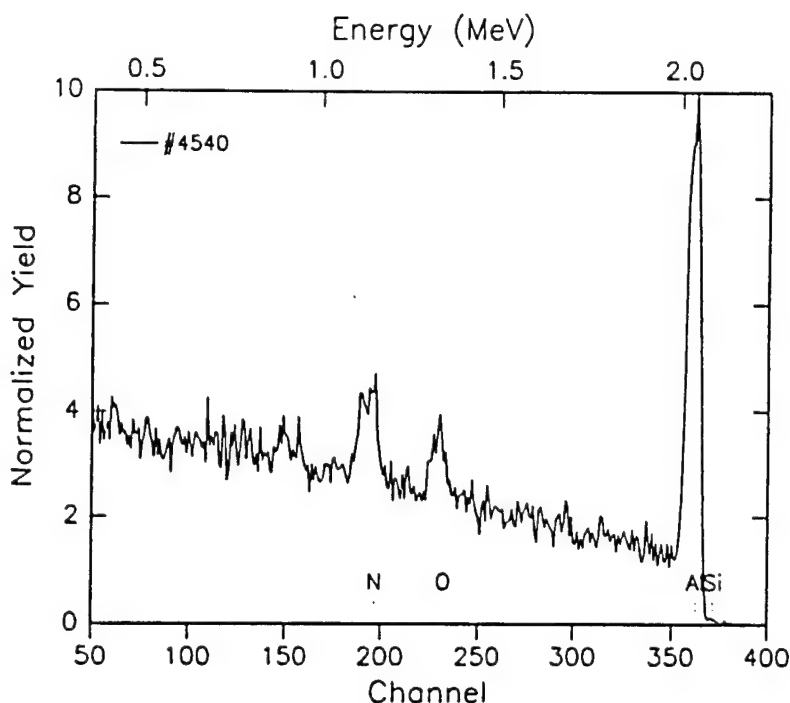


Figure 2. RBS spectrum of a film containing Al and N, grown at room temperature. The O peak is caused by the oxidation of the Al metal during sample transfer from the microwave chamber to the RBS chamber. Growth time: 20 min. Pressure in reaction chamber:  $4.5\text{E-}6$  mbar.

The following procedure was used during the experiments: After flashing the Si substrate to  $> 1000^\circ\text{C}$  for about 1 min, it was cooled down to the growth temperature. After starting the microwave, the pressure in the reaction chamber increased briefly to  $10^{-4}$  mbar. After the discharge became stable, the pressure was reduced and heating of the Ga source was started. This took about 5 min after which the shutter of the effusive cell was opened. After growth was completed, the shutter was closed and the Ga source was allowed to cool down. Then the microwave was turned off and the leak valve for the gas supply was closed. Due to the small diameter of the aperture it took several minutes until the pressure in the reaction chamber returned to  $\leq 10^{-6}$  mbar. Only after the hydrogen peak in the residual gas spectrum had returned to its normal value that the substrate heating was turned off.

For substrate temperature below  $615^\circ\text{C}$ , Ga sticks very efficiently and the resulting films contain much more Ga than a stoichiometric GaN film. The RBS spectrum of a film grown at this temperature is shown in Fig. 3 (solid line). A simulated spectrum of a stoichiometric GaN film which contains the detected amount of Ga is included (dashed line). The measured N peak

is much smaller than the simulated peak indicating that the film is N deficient, i.e. not stoichiometric.

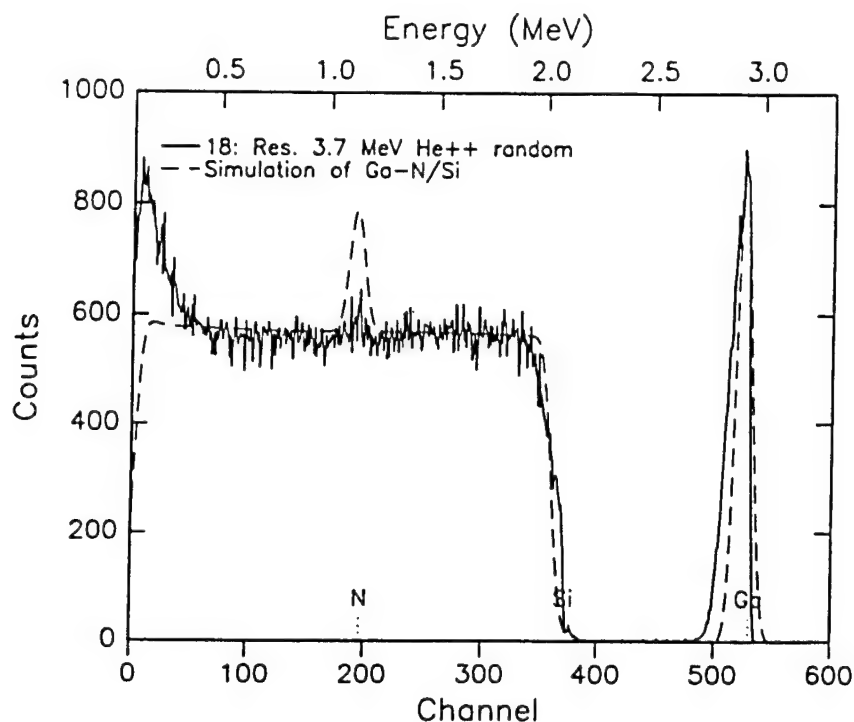


Figure 3. RBS spectrum of a film grown at  $<615^{\circ}\text{C}$  (solid line). The dashed line shows a simulated spectrum of a stoichiometric GaN film of a thickness comparable to the measured Ga intensity. Growth time: 90 min. Pressure in reaction chamber:  $1\text{E-}6$  mbar.

At temperatures above  $665^{\circ}\text{C}$ , Ga desorption becomes dominant, thus limiting the amount of Ga which can be incorporated into the growing film. Films grown in such high temperatures are—at the current growth time of 60-120 min per film—too thin for analysis by RBS. Figure 4 shows the RBS spectrum of such a film grown on Si(100). Due to the small thickness of the film, the Ga peak was barely visible and the N peak cannot be distinguished from the Si background.

Fig. 5 shows the RBS spectrum of a film grown at  $\sim 640^{\circ}\text{C}$ , the temperature at which the best films have been grown so far. The dashed line in Fig. 5 shows the simulation of a GaN film of  $95\text{\AA}$  thickness, assuming a stoichiometry of  $\text{Ga:N}=1:1$ . This simulation fits the measured data quite well. However, the signal-to-background ratio around the N peak is still too low to positively confirm stoichiometry. A thicker film is needed for this purpose.

The typical microwave power is 30-50W. Higher input power tends to heat up the Pyrex tube which would cause it to break. Lower input power leads to unstable discharge conditions.



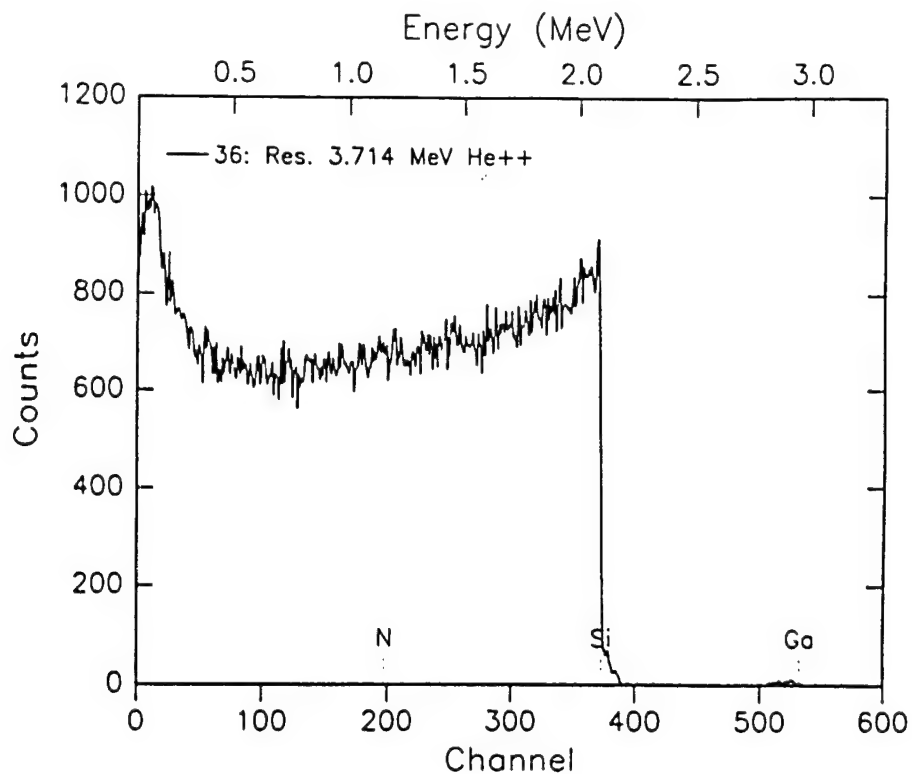


Figure 4. RBS spectrum of a film grown at  $< 665^{\circ}\text{C}$ . Growth time: 120 min. Pressure in reaction chamber:  $2\text{E-}5$  mbar.

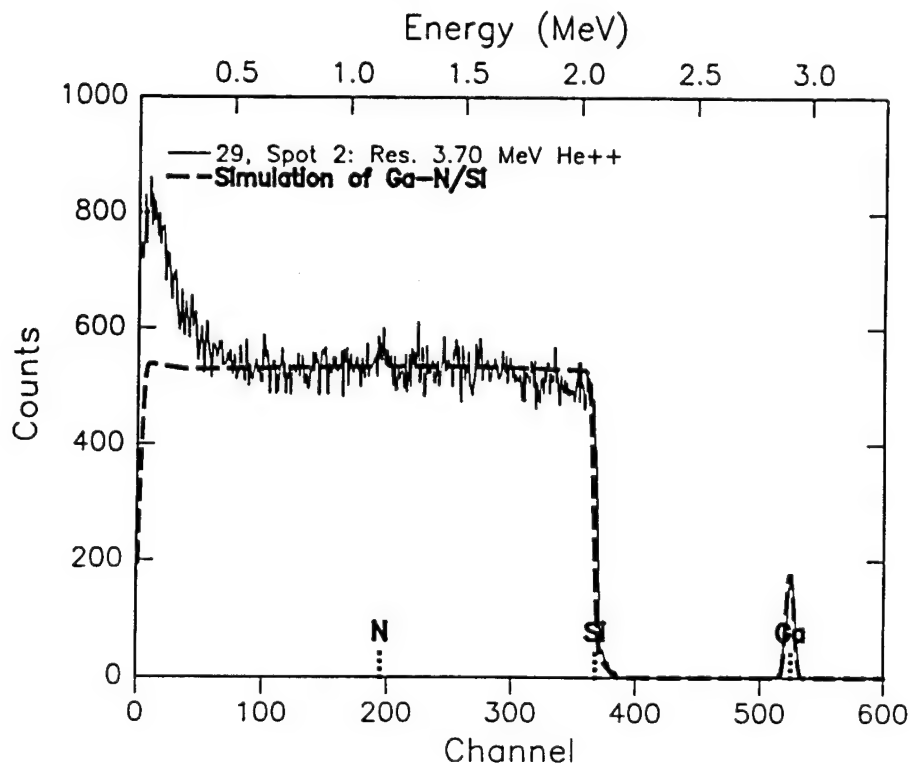


Figure 5. RBS spectrum of a GaN film grown at  $\sim 640^{\circ}\text{C}$  (solid line). The dashed line is a simulated spectrum of a stoichiometric GaN film containing the same amount of Ga as measured on the sample. Growth time: 70 min. Pressure in reaction chamber:  $1.5\text{E-}5$  mbar.

#### D. Conclusions

The successful growth of AlN and GaN shows that the microwave approach works even under LEEM compatible conditions, i.e. pressures  $\leq 10^{-5}$  mbar. However, more tests are necessary and thicker films need to be grown for RBS to confirm stoichiometry.

#### E. Future Research Plans and Goals

After the optimum parameters for GaN growth are established the microwave will be transferred to the LEEM, which will enable us to study the initial stages of the growth of thin films *in situ*. Of special interest is the question of the influence of a possible nitridation of the substrate surface prior to the film growth [2] where LEEM can provide an answer.

The problem of the poor signal-to-background ratio and the N peak in the RBS spectrum will be addressed by switching from Si(100) samples to HOPG, where the N peak would be clearly distinguishable from the C signal since C is lighter than N. When nitride film is conducted in the LEEM, we expect to use  $\alpha$ -SiC(0001) substrates.

#### F. References

1. M. J. Paisley, Z. Sitar, J. B. Posthill, and R. F. Davis, J. Vac. Sci. Technol. A **7**, 701, (1989)
2. H. Okumura, S. Misawa, T. Okahisa, and S. Yoshida, J. Crystal Growth **136**, 361 (1994)
3. S. Meikle, H. Nomura, Y. Nakanishi, and Y. Hatanaka, J. Appl. Phys. **67**, 483 (1990)
4. N. Newman, J. Ross, and M. Rubin, Appl. Phys. Lett. **62**, 1242 (1993)

## IV. Design of a Supersonic Molecular Beam Source for *in situ* Growth of AlN and GaN Layers for Low Energy Electron Microscopy (LEEM)

### A. Introduction

The nitride family of AlN, GaN and InN thin films have shown to be strong candidates for electronic and optoelectronic applications. With direct band gaps of 6.2 eV, 3.4 eV and 1.9 eV for AlN, GaN and InN respectively, solid solutions based on these materials provide for band gap modifications suitable for applications ranging from the red to the deep UV region of the spectrum [1]. However the growth of single crystal, epitaxial films with low defect densities has proven to be troublesome. As deposited GaN shows n-type behavior. It has been proposed that this n-type behavior is due to N vacancies [2]. These vacancies are formed during growth due to the high temperature required to decompose N sources such as NH<sub>3</sub> and to obtain high enough surface mobilities such that a single crystal film is achieved. N sources such as cold cathode ion guns [3] and microwave discharges [4,5] have been used to dissociate N<sub>2</sub> and N<sub>2</sub>/NH<sub>3</sub> mixtures respectively and allow low temperature (i.e. 650°C) growth of GaN. However it has been shown that high temperature anneals will improve the carrier density and crystallinity of the films [6]. Therefore a technique which would provide a N source with a low decomposition temperature and high surface mobility is required to overcome these difficulties.

Supersonic Molecular Beam Epitaxy (SMBE) has been shown to enhance the surface decomposition of silane and methane [7,8]. This is due to the possibility of tuning the kinetic energy of these species such that bond cleavage and deformation occurs upon contact with the substrate. If the kinetic energy available is higher than the barrier for chemisorption on these surfaces, some of the remaining energy can be used to enhance surface diffusion via the generation of surface phonons or the use of surface kinetic energy by part of the adsorbate. SMBE also provides for the tuning of the energy spreads. This is important in order to experimentally determine the chemisorption barriers for the systems being studied as well as to provide species with high sticking coefficients at high enough intensities. SMBE is therefore a suitable technique for the growth of single crystal GaN films at suitable growth rates. A review of Supersonic Molecular Beams can be found in Scoles [9].

The present report entails the design and construction of a Supersonic Molecular Beam Source to be interfaced with the Low Energy Electron Microscope at Arizona State University. This will allow for the study of the growth mechanisms as well as defect evolution during the deposition of GaN and AlN. The ability of such *in situ* analysis will further the development of these films by providing instant feedback on the atomic processes involved during the deposition of these films.

## B. Experimental Procedure

At the present moment the source chamber for deposition of the films is under construction. It will be delivered in the month of November. A gas manifold, described in the previous progress report, has been assembled and is ready to be tested. This will be done in the He atom scattering chamber. This chamber is equipped with the necessary equipment to obtain time of flight data. This data will be used to obtain the mean kinetic energy as well as the energy distribution of the beam as a function of composition, temperature and Pd (stagnation pressure multiplied by the nozzle diameter). The beam characteristics obtained will be compared to those calculated using a binary monoatomic model.

## C. Future Work

The beam characteristics will be determined. This data will be used to optimize the beam energy as well as the energy spread. The source chamber will be tested and preliminary depositions will be performed.

## D. References

1. S. Strite, H. Morkoc, J. Vac. Sci. Technol. B. **10** (4), July/Aug. 1992.
2. A. Estes Wickenden, D. K. Wickenden, T. J. Kistenmacher, J. Appl. Phys. **75**(10), 15 May 1994.
3. Z. Q. He, X. M. Ding, X. Y. Hou, Xun Wang, Appl. Phys. Lett. **64**(3), 17 Jan. 1994.
4. M. J. Paisley, Z. Sitar, J. B. Posthill, R. F. Davis, J. Vac. Sci. Technol. A **7**(3), 17 Jan. 1994.
5. H. Okumura, S. Misawa, T. Okahisa, S. Yoshida, J. Cryst. Growth **136** (1994), 361-365.
6. D. K. Wickenden, J. A. Miragliotta, W. A. Bryden, T. J. Kistenmacher, J. Appl. Phys. **75**(11), 1 June 1994, 7585-87.
7. M. E. Jones, L. Q. Xia, N. Maity, J. R. Engstrom, Chem. Phys. Lett. **229** (1994), 401-407.
8. S. T. Ceyer, J. D. Beckerle, M. B. Lee, S. L. Tang, Q. Y. Yang, M. A. Hines, J. Vac. Sci. Technol. A **5**(4), July/Aug. 1987.
9. D. R. Miller, *Atomic and Molecular Beam Methods*, Ch. 2, Ed. G. Scoles, 1988, Oxford University Press.

## V. Design of System for Deposition of GaN and SiC Films by Dual Colutron Ion Beams

### A. Introduction

The goal of this work is to produce crystalline SiC and GaN films by depositing the chemical components by two ion beams simultaneously. The ion sources are each equipped with a Wien filter to select the mass of the ions. By using electrostatic deceleration lenses, the ion energy can be selected in the 10 eV range with an energy spread as low as 0.1 eV.

The growth process is monitored during the ion deposition by a reflection high-energy electron diffraction (RHEED) system. A retarding field analyzer is used to examine the structure and composition of the deposited films *in situ* by low-energy electron diffraction (LEED) and Auger electron spectroscopy (AES).

### B. Experimental Procedure

The setup of the ion beam deposition system is depicted in Fig. 1. The main chamber houses the equipment to characterize the ion beams (Faraday cup to determine the fluence and beam profile and electrostatic analyzer to measure the ion energy) and the RHEED system to monitor the film growth *in situ*. The Faraday cup and the substrate are mounted in the center axis of the chamber on a high-precision manipulator. The substrate can be heated by applying a direct current. The temperature is measured with an infrared pyrometer through a calcium fluoride window.

The two Colutron ion sources are connected to the main chamber through gate valves. Both ion sources are equipped with electrostatic lenses to form the ion beam and with a Wien filter to select the mass of the ions. One of the sources can be used either for carbon or nitrogen ions (by using CO or N<sub>2</sub> as source gas), the other ion source is equipped with a BN source crucible to produce either gallium or silicon ions from the elements.

Deflection units inside the main chamber, directly in front of the deceleration lenses, separate the ions from energetic neutrals. The neutrals are accelerated ions which were neutralized by collisions in the Colutron chamber. These particles are not decelerated by the electrostatic lenses and would cause damage to the grown films on the substrate. Therefore, a deflection of the ion beam by an electric field into the deceleration lens is necessary to prevent neutrals from reaching the target. This is achieved by deflecting the ion beam 2° off the ion source axis. Inside the chamber, directly in front of the substrate (30 mm distance between substrate and the end of the lens), the deceleration lenses retard the ions to the required low energies. The ion beams impinge on the substrate at an angle of 30° with respect to the surface normal.

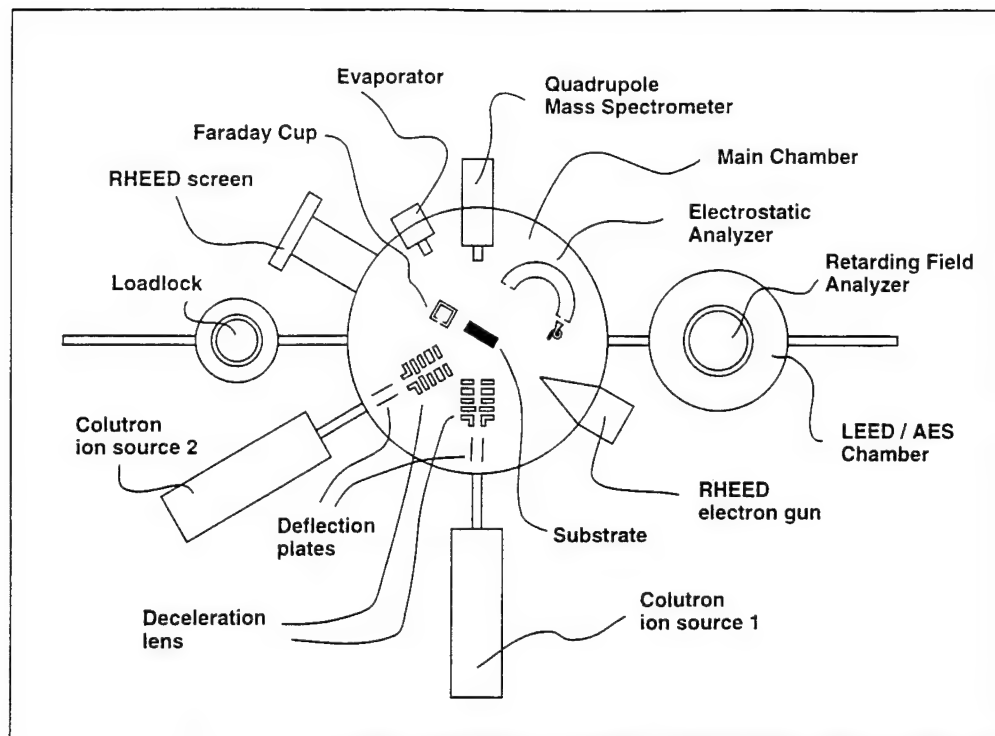


Figure 1. Schematic drawing of the dual Colutron ion beam deposition experiment. The setup consists of a loadlock, the main chamber connected to the two Colutron ion sources and a LEED/AES chamber.

The RHEED gun produces an electron beam with an energy up to 10 keV which impinges on the substrate at a grazing angle. The fluorescent screen is located on the opposite chamber side, with the axis shifted along the sample normal. Due to this shift of the screen a larger portion of the diffraction image is observable. The RHEED system is primarily used to monitor the layer growth. For a layer-by-layer film growth, oscillations in the RHEED spot intensities occur. When a new layer is completed, the surface is smooth and the reflected intensity has a maximum. At a maximum disorder on the surface, which corresponds to the growth of half a new layer, the reflected intensity shows a minimum. A second application of the RHEED equipment is the determination of the structure of the grown layer.

The main chamber is also equipped with a quadrupole mass spectrometer which enables a residual gas analysis and hereby monitoring the species present in the residual gas. A silicon evaporator provides a source of silicon which prevents the depletion of Si in SiC substrate surfaces during the cleaning procedure. The main chamber is pumped by a turbomolecular pump and an additional titanium sublimation pump, which is cooled with liquid nitrogen. After bakeout, a total pressure of less than  $1 \times 10^{-10}$  torr is expected.

The loadlock chamber is separated from the main chamber by a gate valve and is separately pumped by a turbomolecular pump. It enables a quick sample loading without breaking the vacuum in the main chamber.

The LEED/AES chamber is also connected to the main chamber through a gate valve and is separately pumped by a turbomolecular pump. It enables a quick sample loading without breaking the vacuum in the main chamber.

The LEED/AES chamber is also connected to the main chamber through a gate valve. The retarding field analyzer enables both structural analysis of the outermost film layers by means of LEED and the compositional analysis in the depth range of several monolayers by Auger electron spectroscopy. The chamber is pumped by an oil diffusion pump, which is equipped with a liquid nitrogen cold trap to reduce the hydrocarbon contamination of the vacuum.

The sample transfer between all three chambers is possible by using magnetically coupled transfer feedthroughs. In the LEED/AES chamber, a high-precision feedthrough is used to enable an exact sample positioning in front of the retarding field analyzer.

#### C. Results

The construction ion beam deposition chamber, the loadlock and the LEED/AES chamber has been completed. Assembly of the apparatus is in progress.

#### D. Future Research Plans and Goals

After the assembly of the vacuum system, the ion sources will be tested and the ion beams will be characterized. The LEED and AES data acquisition system will be assembled. For the AES analysis, a computer program has to be adapted to the experimental setup. After the successful test of the equipment, SiC films will be deposited. Analysis of these films will be performed *in situ* by RHEED, LEED and AES and *ex situ* by RBS and LEEM. In a later stage, the production of GaN films on SiC substrates is planned.



## VI. Surface Microstructure and Crystal Structure of 6H-SiC(0001) Substrates for Nitride Film Growth

### A. Introduction

As pointed out in our previous progress report (June, 1995), commercially available SiC crystals are generally not defect-free. In order to conduct meaningful studies by LEEM, these defects must be minimized. The chemical etching procedure described in the previous report did not lead to the desired success. We have, therefore, explored various other ways and used LEEM and LEED to characterize the 6H-SiC(0001) substrate surface.

### B. Siemens Process

Siemens (Erlangen, Germany) uses an undisclosed high-temperature process for the preparation of 6H-SiC(0001) surfaces for epitaxial growth. We have sent, on different occasions, 6H-SiC(0001) n- and p-type samples purchased from Cree Research to Siemens for treatment. The results were irreproducible, despite nominally identical treatments. The treated samples were very heterogeneous with pronounced polytype formation. The number of samples was not large enough to allow statistically significant conclusions. When the as-received samples from Cree were examined in the LEEM, they gave a poor or no LEED patterns which could, however, be improved by heating to several hundred degrees. The microstructure, however, could not be improved noticeably. Surfaces were found to contain scratches or etch pits or both. Two test crystals were sent to NASA Ames Lewis Research Center which also uses a high-temperature surface preparation procedure, but these have not yet been returned. For all these reasons, we have decided to add a standard Si surface preparation procedure, the RCA cleaning treatment.

### C. RCA cleaning

This procedure is based on the original RCA [1] cleaning procedure for silicon, with the added degreasing step:

- Blow away large particles from the sample with clean, filtered and dry nitrogen.

- Immerse samples 5 minutes in boiling 1,1,1-trichlorethane.

- Immerse samples 5 minutes in boiling acetone.

- Immerse samples 5 minutes in boiling isopropyl alcohol.

- Rinse samples in DI water for at least 5 minutes.

- Immerse samples 20 minutes at a temperature of 75°C in 5:1:1 H<sub>2</sub>O(DI)-H<sub>2</sub>O<sub>2</sub>(30% unstabilized)-NH<sub>4</sub>OH(27%).

- Quench and rinse in running DI water for at least 5 minutes.

- Immerse samples 20 minutes at a temperature of 75°C in 6:1:1 H<sub>2</sub>O(DI)-H<sub>2</sub>O<sub>2</sub>(30% unstabilized)-HCL(37%).

Quench and rinse in running DI water for at least 5 minutes.

Dry samples with clean and filtered nitrogen, or spin dry.

Both the two Siemens-treated crystals and an as-received epilayer crystal were subjected to this process.

#### D. LEED/LEEM Studies

Both Siemens-treated crystals showed a  $(1 \times 1)$  pattern after mild heating ( $\sim 500^\circ\text{C}$ ). On one crystal the pattern was very strong and persisted with little background even after a brief exposure to air. The spot to background ratio improved with increasing annealing temperature until at about  $1000^\circ\text{C}$  a  $(\sqrt{3} \times \sqrt{3})$   $R30^\circ$  pattern appeared. In one sample the  $(\sqrt{3} \times \sqrt{3})$  pattern appeared simultaneously with a  $(3 \times 1)$  pattern as shown in Fig. 1(a) while in the other, the  $(3 \times 1)$  was absent. The  $(3 \times 1)$  pattern was occasionally stronger than the  $(\sqrt{3} \times \sqrt{3})$  pattern as in Fig. 1(b). These patterns improved up to about  $1150^\circ\text{C}$  and then rapidly deteriorated with further increasing temperature.

The evolution of the LEED pattern of the as-received epilayer sample was studied as a function of temperature. A diffuse  $(\sqrt{3} \times \sqrt{3})$   $R30^\circ$  pattern with strong background became visible after mild heating ( $\sim 500^\circ\text{C}$ ) which improved with increasing annealing temperature up to about  $1100^\circ\text{C}$ . When the temperature was further increased slightly, the  $(\sqrt{3} \times \sqrt{3})$  pattern was displaced by a satellite pattern as shown in Fig. 1(c) which deteriorated above  $1150^\circ\text{C}$ . LEEM images of the epilayer surface showed no scratches, but with very fine grains. No noticeable changes with annealing temperature could be observed in the LEEM, contrary to the Siemens-treated samples without epilayers.

The surfaces of the two Siemens-treated crystals had many scratches which appeared to become wider and shallower with increasing temperature but could not be removed even at the highest temperature studied ( $1150^\circ\text{C}$ ) beyond which the LEED pattern showed only weak  $(1 \times 1)$  spots and  $\langle 10 \rangle$  streaks on a strong background, with extensive disordering. In addition to the scratches, a grain structure is observed whose intensity oscillates strongly with electron energy indicating the coexistence of at least two polytypes. This is illustrated in Fig. 2(a)-(c). These images have a field of view of  $7\mu\text{m}$  and were recorded at 45.8 eV, 49.4 eV and 52.5 eV, respectively. In Fig. 2(a) and 2(c) the domain contrast reverses, while in Fig. 2(b) where the electron energy is in between those in 2(a) and 2(c), only some of the scratches and contamination particles are visible and the domain contrast greatly reduced. Upon a slight defocus of Fig. 2(b), many more shallower scratches came into view.

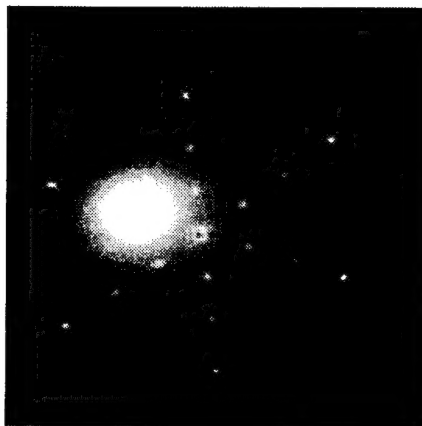
#### E. Conclusions

The RCA procedure cleans the surface to the extent that mild heating reveals the lateral periodicity of the surface. However, it does not remove the scratches and it produces

(a)



(b)



(c)

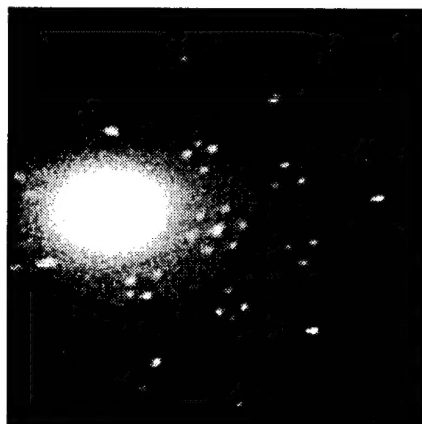
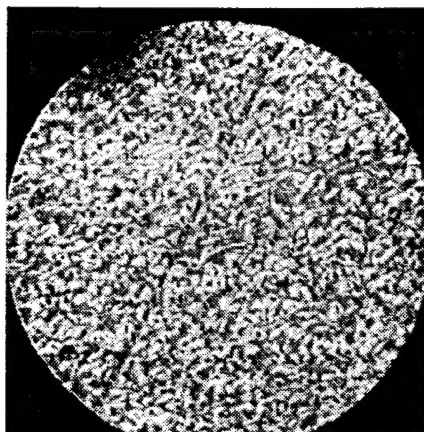
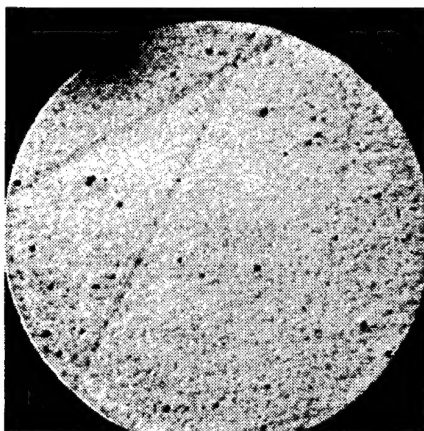


Figure 1. (a) A  $(\sqrt{3} \times \sqrt{3})$  R30° LEED pattern with also  $(3 \times 1)$  spots. Electron energy = 4 3.4 eV.  
(b) A  $(3 \times 1)$  LEED pattern. Electron energy = 30.2 eV.  
(c) A  $(\sqrt{3} \times \sqrt{3})$  LEED pattern with satellite spots. Electron energy = 41.3 eV

(a)



(b)



(c)

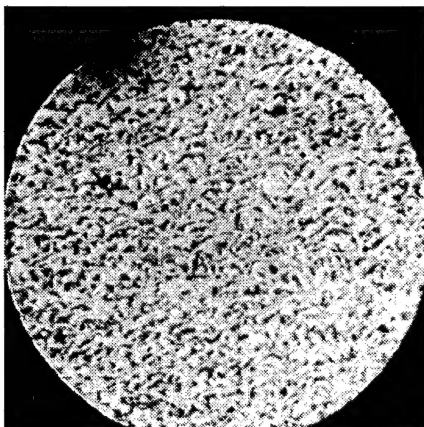


Figure 2. LEEM images of the 6H-SiC(0001) surface as a function of electron energy. (a) 45.8eV, (b) 49.4eV and (c) 52.5eV. A contrast reversal is observed in (a) and (c). Field of view = 7.0  $\mu\text{m}$ .

particulate contamination (see dark spots in LEEM images in Fig. 2). Whether or not the polytype domain structure of the Siemens-treated crystals is caused by the high-temperature process used or already present in the as-delivered samples must still be determined by comparative experiments. The epilayer crystals are scratch-free but have a inferior crystal perfection. At present it appears that (a) RCA cleaning removes surface contamination sufficiently for LEED/LEEM studies, and (b) the Siemens process cannot remove scratches without inducing polytype formation. As a consequence, the RCA cleaning procedure of as-received Cree crystals may be adequate for use as epitaxy substrates if Cree can reduce the scratch density. Further studies are necessary, however, in order to accumulate statistically significant information.

#### F. References

1. W. Kern and D. A. Puotinen, RCA Rev. **31**, 187 (1970).

## VII. Distribution List

Mr. Max Yoder Office of Naval Research Electronics Division, Code: 312 Ballston Tower One 800 N. Quincy Street Arlington, VA 22217-5660	3
Administrative Contracting Officer Office of Naval Research Regional Office Atlanta 101 Marietta Tower, Suite 2805 101 Marietta Street Atlanta, GA 30323-0008	1
Director, Naval Research Laboratory ATTN: Code 2627 Washington, DC 20375	1
Defense Technical Information Center Bldg. 5, Cameron Station Alexandria, VA 22304-6145	2